Mineralogical Magazine (2024), **88**, 369–379
doi:10.1180/mgm.2024.26

Article

Amableite-(Ce), $Na_{15}[(Ce_{1.5}Na_{1.5})Mn_3]Mn_2Zr_3\square Si[Si_{24}O_{69}(OH)_3](OH)_2\cdot H_2O$, a new eudialyte-group mineral from Saint-Amable Sill, Québec, Canada

Nikita V. Chukanov[1,2], Andrey A. Zolotarev[3], Christof Schäfer[4], Dmitry A. Varlamov[5], Igor V. Pekov[2], Marina F. Vigasina[2], Dmitry I. Belakovskiy[8], Sergey M. Aksenov[6,7], Svetlana A. Vozchikova[1] and Sergey N. Britvin[3]

[1]Federal Research Center of Problems of Chemical Physics and Medicinal Chemistry, Russian Academy of Sciences, Chernogolovka, Moscow region, 142432 Russia; [2]Faculty of Geology, Moscow State University, Vorobievy Gory, 119991 Moscow, Russia; [3]Department of Crystallography, St. Petersburg State University, University Emb. 7/9, Saint-Petersburg 199034, Russia; [4]Independent researcher, Untereisesheim, Germany; [5]Institute of Experimental Mineralogy RAS, Chernogolovka, 142432 Russia; [6]Laboratory of Arctic Mineralogy and Material Sciences, Kola Science Centre, Russian Academy of Sciences, 14 Fersman str., Apatity 184209 Russia; [7]Geological Institute, Kola Science Centre, Russian Academy of Sciences, 14 Fersman str., Apatity 184209 Russia; and [8]Fersman Mineralogical Museum of the Russian Academy of Sciences, Leninsky Prospekt 18-2, 119071 Moscow, Russia

Abstract

The new eudialyte-group mineral amableite-(Ce), ideally $Na_{15}[(Ce_{1.5}Na_{1.5})Mn_3]Mn_2Zr_3\square Si[Si_{24}O_{69}(OH)_3](OH)_2\cdot H_2O$, was discovered in a peralkaline pegmatite at Saint-Amable Sill, Montérégie, Québec, Canada. The associated minerals are albite, microcline, aegirine, serandite, natrolite, yofortierite, and an unidentified titanosilicate forming minute grains. Amableite-(Ce) occurs as yellow equant or thick tabular crystals up to 2 mm across. The observed crystal forms are {0001}; the subordinate forms are {11$\bar{2}$0}, {10$\bar{1}$1}, and {10$\bar{1}$0}. Amableite-(Ce) is brittle, with a Mohs hardness of 5. D(meas) = 2.89(1), D(calc) = 2.899 g·cm^{-3}. Amableite-(Ce) is optically anomalously biaxial (+) with $\alpha \approx \beta = 1.603(2)$ and $\gamma = 1.608(2)$. The chemical composition is (wt.%, electron microprobe, H_2O measured by means of a modified Penfield method): Na_2O 14.20, K_2O 0.41, CaO 1.89, MnO 8.25, Fe_2O_3 2.40, La_2O_3 3.10, Ce_2O_3 4.19, Pr_2O_3 0.16, Nd_2O_3 0.59, SiO_2 49.41, ZrO_2 11.17, HfO_2 0.24, TiO_2 0.68, Nb_2O_5 1.54, Cl 0.26, H_2O 1.70, –O≡Cl –0.06, total 100.13. The crystal structure was determined using single-crystal X-ray diffraction data and refined to $R_1 = 0.0423$. Amableite-(Ce) is trigonal, space group $R3$, with $a = 14.1340(3)$ Å, $c = 30.3780(11)$ Å and $V = 5255.6(3)$ Å^3. The crystal-chemical formula is $(Na_{12.93}K_{0.27}Ce_{0.06})_{\Sigma 13.26}[(Mn_{2.49}Ce_{0.30}Ca_{0.21})_{\Sigma 3.00}(Ce_{1.14}Na_{1.04}Ca_{0.82})_{\Sigma 3.00}](Mn_{1.05}Fe_{0.90}\square_{1.05})_{\Sigma 3.00}(Zr_{2.85}Ti_{0.12}Hf_{0.03})_{\Sigma 3.00}(\square_{0.40}Nb_{0.36}Si_{0.24})_{\Sigma 1.00}(Si_{0.88}\square_{0.12})_{\Sigma 1.00}[Si_{24}(O_{70.44}(OH)_{1.56})_{\Sigma 72.00}][(OH)_{2.20}(H_2O)_{1.27}]_{\Sigma 3.47}Cl_{0.22}$ ($Z = 3$). Infrared and Raman spectra are given. The strongest lines of the powder X-ray diffraction pattern [d, Å (I, %)(hkl)] are: 11.34 (51)(101), 7.06 (76)(110), 4.312 (63)(205), 3.783 (38)(033), 3.538 (43)(027, 220), 2.963 (84)($\bar{3}$45), 2.837 (100)(404). The mineral is named after the discovery locality.

Keywords: amableite-(Ce); new mineral; eudialyte group; crystal structure; IR spectroscopy; Raman spectroscopy; X-ray diffraction; Saint-Amable Sill; Canada

(Received 2 February 2024; accepted 30 March 2024; Accepted Manuscript published online: 12 April 2024)

Introduction

Eudialyte-group minerals (EGMs) are important components of some types of peralkaline rocks in which they are the main concentrators of zirconium. Currently, 32 mineral species belonging to the eudialyte group are known (https://www.mindat.org/). Their crystal structures are based on heteropolyhedral frameworks composed of nine- and three-membered rings of SiO_4 tetrahedra, six-membered rings of edge-sharing $M1O_6$ octahedra and isolated ZO_6 octahedra. The simplified general formula of EGMs is $[N1N2N3N4N5]_3M1_6M2_3M3M4Z_3(Si_9O_{27})_2(Si_3O_9)_2\text{Ø}_{4-6}X1X2$ where $N1$–5 are extra-framework cations (mainly, Na^+ or H_3O^+, sometimes with species-defining H_2O, K^+, Ca^{2+}, Sr^{2+}, Mn^{2+} or REE^{3+} as well as minor H^+ and/or Ba^{2+}); $M1 = Ca^{2+}$, Na^+, Fe^{2+}, Mn^{2+} and REE^{3+}; $M2 = Na^+$, Fe^{2+}, Mn^{2+}, Fe^{3+} or Zr, occurring between rings of $M1O_6$ octahedra; $M3$ and $M4$ are $^{[4]}$Si, $^{[4]}$Nb, $^{[4]}$W or $^{[4]}$Ti atoms occurring at the centres of the Si_9O_{27} rings; Z = Zr or Ti; Ø, $X1$ and $X2$ are additional extra-framework cations (OH^-, Cl^-, F^-, O^{2-}, CO_3^{2-}, SO_4^{2-} and S^{2-}) and water molecules (Johnsen *et al.*, 2003; Rastsvetaeva *et al.*, 2012). All sites except those belonging to the rings of tetrahedral and octahedra can be partly vacant. Most EGMs are characterised by the space groups $R\bar{3}m$ or $R3m$, but in some species (members of the oneillite subgroup) different $M1$ cations are ordered in the $M1(1)$ and $M1(2)$ sites alternating in the six-membered rings of octahedra which results in lowering of symmetry from $R\bar{3}m$ or $R3m$ to $R3$ (Johnsen *et al.*, 1999; Chukanov *et al.*, 2003, 2020, 2022, 2023; Khomyakov *et al.*, 2007, 2009).

Corresponding author: Nikita V. Chukanov; Email: chukanov@icp.ac.ru
Associate Editor: Daniel Atencio
Cite this article: Chukanov N.V., Zolotarev A.A., Schäfer C., Varlamov D.A., Pekov I.V., Vigasina M.F., Belakovskiy D.I., Aksenov S.M., Vozchikova S.A. and Britvin S.N. (2024) Amableite-(Ce), $Na_{15}[(Ce_{1.5}Na_{1.5})Mn_3]Mn_2Zr_3\square Si[Si_{24}O_{69}(OH)_3](OH)_2\cdot H_2O$, a new eudialyte-group mineral from Saint-Amable Sill, Québec, Canada. *Mineralogical Magazine* **88**, 369–379. https://doi.org/10.1180/mgm.2024.26

This paper describes a new oneillite-subgroup member amableite-(Ce), with $Na^{+} + REE^{3+}$ and Mn^{2+} ordered in the *M*1(1) and *M*1(2) sites and Mn^{2+}-dominant *M*2 site. Amableite-(Ce) is named after its discovery locality, Saint-Amable Sill. The mineral and its name (with symbol Ambl-Ce) have been approved by the Commission on New Minerals, Nomenclature and Classification of the International Mineralogical Association (IMA2023–075, Chukanov *et al.*, 2024). The holotype specimen is deposited in the Fersman Mineralogical Museum of the Russian Academy of Sciences, Moscow, Russia with the registration number 6921/1.

Experimental methods and data processing

In order to obtain infrared (IR) absorption spectra of amableite-(Ce) and the related eudialyte-group mineral voronkovite (Khomyakov *et al.*, 2009), powdered samples were mixed with anhydrous KBr, pelletised, and analysed using an ALPHA FTIR spectrometer (Bruker Optics) at a resolution of 4 cm^{-1}. A total of 16 scans were collected. The IR spectrum of an analogous pellet of pure KBr was used as a reference. The assignment of IR bands was made based on the analysis of IR spectra of several tens of structurally investigated eudialyte-group minerals, in accordance with Rastsvetaeva *et al.* (2012).

Raman spectra of randomly oriented grains of amableite-(Ce) and other eudialyte-group minerals used for comparison were obtained using an EnSpectr R532 spectrometer based on an OLYMPUS CX 41 microscope coupled with a diode laser ($\lambda = 532$ nm) at room temperature (Moscow State University, Faculty of Geology). The spectra were recorded in the range from 100 to 4000 cm^{-1} with a diffraction grating (1800 gr mm^{-1}) and spectral resolution of ~6 cm^{-1}. The output power of the laser beam was in the range from 5 to 13 mW. The diameter of the focal spot on the sample was 5–10 μm. The back-scattered Raman signal was collected with a 40× objective; signal acquisition time for a single scan of the spectral range was 1 s, and the signal was averaged over 50 scans. Crystalline silicon was used as a standard.

Compositional data (5 spot analyses) were obtained using a digital scanning electron microscope Tescan VEGA-II XMU equipped with an energy-dispersive spectrometer (EDS) INCA Energy 450 with semiconducting Si (Li) detector Link INCA Energy at an accelerating voltage of 20 kV, electron current of 190 pA and electron beam diameter of 160–180 nm. Attempts to use WDS mode, with a higher beam current, were unsuccessful because of the instability of the mineral under the electron beam due to partial dehydration and migration of Na. This phenomenon is typical for high-hydrous sodium minerals with microporous structures. A good agreement was observed between compositional data obtained under these standard conditions and those obtained under more 'mild' conditions (with a current lowered to 90–100 pA and electron beam defocused to an area of 30 × 30 μm). The *L*-lines of Ta are not observed in the spectrum, which indicates the absence of detectable amounts of tantalum in amableite-(Ce).

The H_2O content was determined by means of a modified Penfield method. The CO_2 content was not determined because characteristic bands of carbonate groups (in the range of 1350–1550 cm^{-1}) are not observed in the IR spectrum of amableite-(Ce).

Powder X-ray diffraction (XRD) data were collected using a Rigaku R-AXIS Rapid II diffractometer (image plate), Co*K*α, 40 kV, 15 mA, rotating anode with the microfocus optics, Debye-Scherrer geometry, $d = 127.4$ mm and exposure time of 15 min. The raw powder XRD data were collected using the program suite designed by Britvin *et al.* (2017). Calculated intensities were obtained by means of *STOE WinXPOW* v. 2.08 program suite based on the atomic coordinates and unit-cell parameters (Stoe, 2003).

Single-crystal X-ray diffraction studies were carried out using a Rigaku XtaLAB Synergy-S diffractometer (Mo*K*α radiation) with high-stability sharp-focus X-ray source PhotonJet-S and a high-speed direct-action detector HyPix-6000HE. *CrysAlisPro* software was used for further processing (CrysAlisPro, 2015). An absorption correction was introduced using the *SCALE3 ABSPACK* algorithm. The obtained data were loaded into the *Olex2* program software (Dolomanov *et al.*, 2009) and the crystal structure was solved and refined by the *ShelX* program package (Sheldrick, 2015). The crystal data, experimental details of the data collection and refinement results are shown in Table 1.

Results

Occurrence, general appearance and physical properties

The material with amableite-(Ce) was collected in the Demix-Varennes quarry, Saint-Amable Sill (45° 40′1″N, 73°20′35″W), Lajemmerais RCM, Montérégie, Québec, Canada (see: Horváth *et al.*, 1998). Amableite-(Ce) crystallised from a peralkaline post-magmatic fluid. It forms yellow thick-tabular, slightly flattened on (0001) crystals up to 2 mm across in cavities of peralkaline pegmatite (Fig. 1). The dominant crystal form is {0001}; the subordinate forms are $\{11\bar{2}0\}$, $\{10\bar{1}1\}$ and $\{10\bar{1}0\}$. The associated minerals are albite, microcline, aegirine, serandite, natrolite, yofortierite, and an unidentified titanosilicate forming minute grains.

Amableite-(Ce) is brittle, with a Mohs hardness of 5. No cleavage is observed. The fracture is uneven. Density measured by

Table 1. Crystal data, data collection information and structure refinement details for amableite-(Ce).

Crystal data	
Crystal system	Trigonal
Space group	*R*3
a (Å)	14.1340(3)
c (Å)	30.3780(11)
V (Å^3)	5255.6(3)
Z	3
μ (mm^{-1})	2.912
F (000)	4398.0
Data collection	
Crystal size (mm)	0.18 × 0.12 × 0.09
Temperature (K)	293(2)
Radiation	Mo*K*α ($\lambda = 0.71073$)
2θ range for data collection (°)	6.792 to 67.286
Index ranges	$-19 \le h \le 21$ $-21 \le k \le 21$ $-41 \le l \le 45$
Reflections collected	12263
Independent reflections	6914 ($R_{int} = 0.0214$, $R_{sigma} = 0.0318$)
Refinement	
Data/restraints/parameters	6914/3/449
Goodness-of-fit on F^2	1.035
Final *R* indexes [$I > 2\sigma(I)$]	$R_1 = 0.0423$, $wR_2 = 0.1120$
Final *R* indexes [all data]	$R_1 = 0.0450$, $wR_2 = 0.1138$
Largest diff. peak/hole (*e*·Å^{-3})	1.31/−1.65
Flack parameter	0.16(2)

https://doi.org/10.1180/mgm.2024.26 Published online by Cambridge University Press

Figure 1. Amableite-(Ce) crystals (yellow) in association with albite, aegirine and natrolite. Field of view width is 3.5 mm. Sample 6921/1 from the Fersman Mineralogical Museum of the Russian Academy of Sciences, Moscow, Russia. Photographer: V. Heck.

flotation in heavy liquids (mixtures of methylene iodide and heptane) is equal to 2.89(1) g·cm^{-3}. Density calculated using the empirical formula and unit-cell volume refined from single-crystal XRD data is 2.90 g·cm^{-3}.

The new mineral is optically anomalously biaxial (+) with $\alpha \approx \beta = 1.603(2)$ and $\gamma = 1.608(2)$ ($\lambda = 589$ nm). Different causes of optical anomalies (microstrains, compositional inhomogeneity, including different degrees of dehydration in different zones or sectors) are discussed in detail by Shtukenberg and Punin (2007). A possible cause of optical anomalies may be deformation of the crystals during their growth or when they were being crushed. In particular, anomalous biaxiality is very typical for eudialyte-group minerals despite that all studied members of this group are trigonal (Rastsvetaeva *et al.*, 2012). Under the microscope, amableite-(Ce) is colourless and nonpleochroic. Dispersion is distinct with $r > v$.

Infrared spectroscopy

Absorption bands in the IR spectrum of amableite-(Ce) (curve *a* in Fig. 2) and their assignments are (cm^{-1}, s – strong band, w – weak band, sh – shoulder): 3520, 3335, 2880w (O–H stretching vibrations); 1635w (H–O–H bending vibrations); 1170sh, 1010s, 991s (Si–O stretching vibrations of silicate rings); 935s (Si–O stretching vibrations of SiO_4 tetrahedra at the *M*3 and *M*4 sites); 739 (mixed vibrations of rings of SiO_4 tetrahedra – 'ring band'); 700sh, 657 (mixed vibrations of rings of SiO_4 tetrahedra combined with Nb–O stretching vibrations); 519sh ($^{IV}Mn^{2+}$–O and/or $^{V}Fe^{3+}$–O stretching vibrations); 481s, 446s (lattice mode involving predominantly bending vibrations of rings of SiO_4

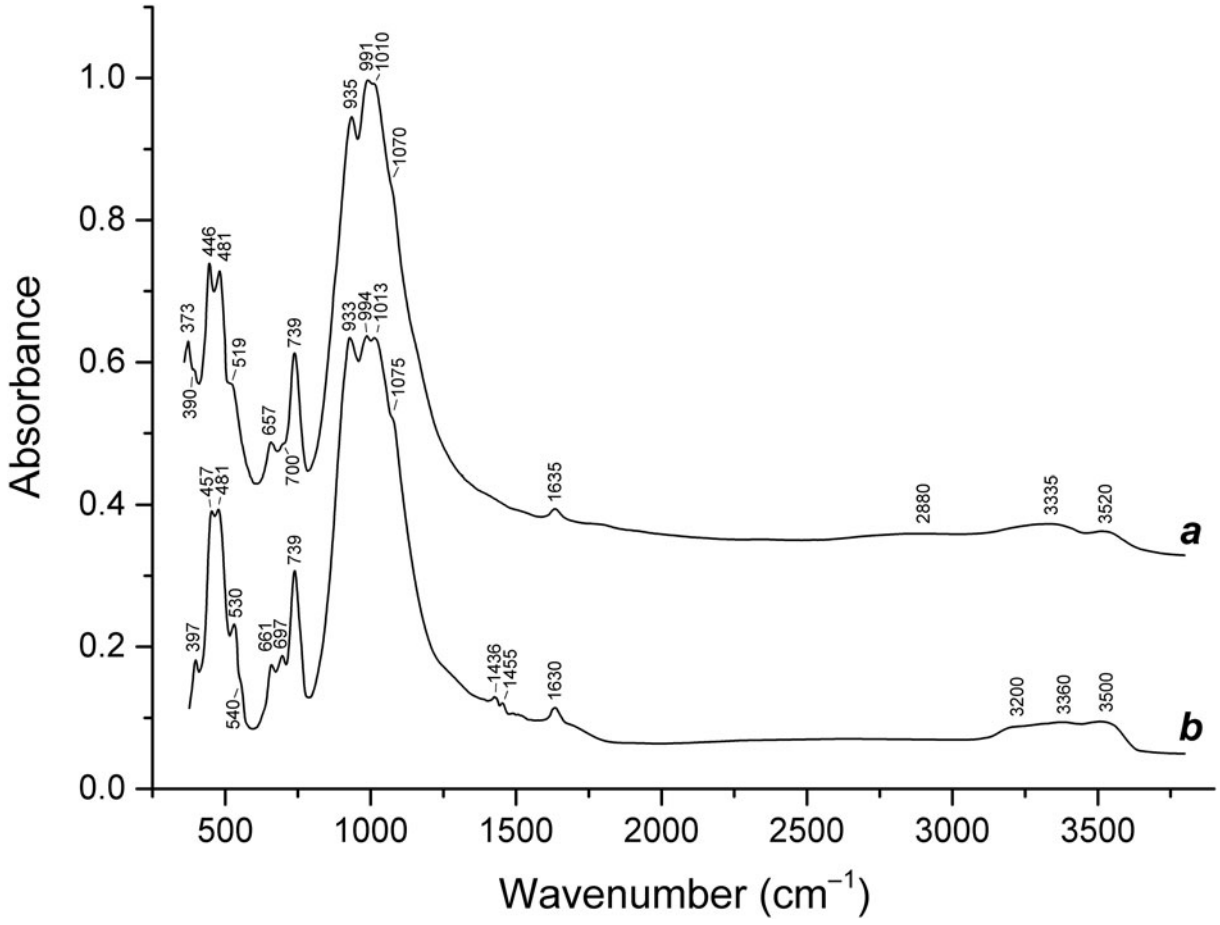

Figure 2. Powder infrared absorption spectra of (*a*) amableite-(Ce) and (*b*) holotype sample of voronkovite (Khomyakov *et al.*, 2009), an oneillite-type EGM related to amableite-(Ce). The spectra are offset for comparison.

https://doi.org/10.1180/mgm.2024.26 Published online by Cambridge University Press

tetrahedra); and 390sh, 373 (lattice modes involving ^{VI}(Ca;Mn^{2+})–O stretching vibrations).

The band of $^{IV}Fe^{2+}$–O stretching vibrations (in the range 539–545 cm^{-1}) was not observed. The IR spectrum of amableite-(Ce) differs from that of the related eudialyte-group mineral voronkovite, ideally $Na_{15}[(Na,Ca)_3Mn_3]Fe_3^{2+}Zr_3Si_2(Si_{24}O_{72})(OH,O)_4Cl{\cdot}H_2O$ (curve *b* in Fig. 2), with a lower intensity of the band at 933–935 cm^{-1}, which reflects significant amounts of vacancies and Nb at the *M*3 and *M*4 sites, in accordance with the structural data (see below).

According to the correlation by Libowitzky (1999), the band of O–H stretching vibrations with the maximum at 3335 cm^{-1} corresponds to a hydrogen bond with the O···O distance of 2.72 Å. Thus, this band should be assigned to the hydrogen bond O24···H–O26 with the O···O distance of 2.72(3) Å. The band at 3520 cm^{-1} may correspond to silanol groups formed as a result of protonation of pending vertices of the SiO_4 tetrahedra, but this assignment is ambiguous because H atoms were not localised.

Raman spectroscopy

A specific feature of Raman spectra of the EGMs selsurtite, ideally $(H_3O)_{12}Na_3(Ca_3Mn_3)(Na_2Fe)Zr_3\square Si[Si_{24}O_{69}(OH)_3](OH)Cl{\cdot}H_2O$ (Chukanov *et al.*, 2023), aqualite, ideally $(H_3O)_9(K,Ba,Sr)_2Ca_6Zr_3Na_2Si_2[Si_{24}O_{66}(OH)_6](OH)_3Cl{\cdot}H_2O$ (Khomyakov *et al.*, 2007) and other hydronium-bearing EGMs is a series of bands in the range of 1200–2900 cm^{-1} corresponding to strong hydrogen bonds formed by hydronium cations in different local situations including Zundel- and Eigen-like bonds with short O···O distances of ~2.4 and ~2.6 Å (Chukanov *et al.*, 2022, 2023; see Discussion section for details). Similar but much weaker bands are observed in the Raman spectrum of amableite-(Ce), but such bands are absent in the Raman spectrum of eudialyte, which does not contain hydrated proton complexes including $(H_3O)^+$ cation groups (Fig. 3). Most probably, hydrated protons could form as a result of partial dissociation of silanol (SiOH) groups.

The assignment of other bands in the Raman spectrum of amableite-(Ce) is as follows: 3430 cm^{-1} to O–H stretching vibrations of H_2O molecules and/or OH groups; the range 900–1300 cm^{-1} to Si–O stretching modes; 780 cm^{-1} to mixed vibrations of rings of SiO_4 tetrahedra; 653 and 689 cm^{-1} to mixed vibrations of rings of SiO_4 tetrahedra combined with Nb–O stretching vibrations; 573 cm^{-1} to Zr–O stretching vibrations and bands ≤ 400 cm^{-1} are assigned to lattice modes.

Chemical data

Analytical data are given in Table 2. Contents of other elements with atomic numbers >8 are below detection limits. Based on IR spectroscopy data, all iron is considered as Fe^{3+}. Note that Fe^{3+} and Fe^{2+} cations at the *M*2 site of eudialyte-group minerals are yellow and red (to brownish-red in the case of five-fold coordination) chromophores, respectively (Pol'shin *et al.*, 1991). Thus,

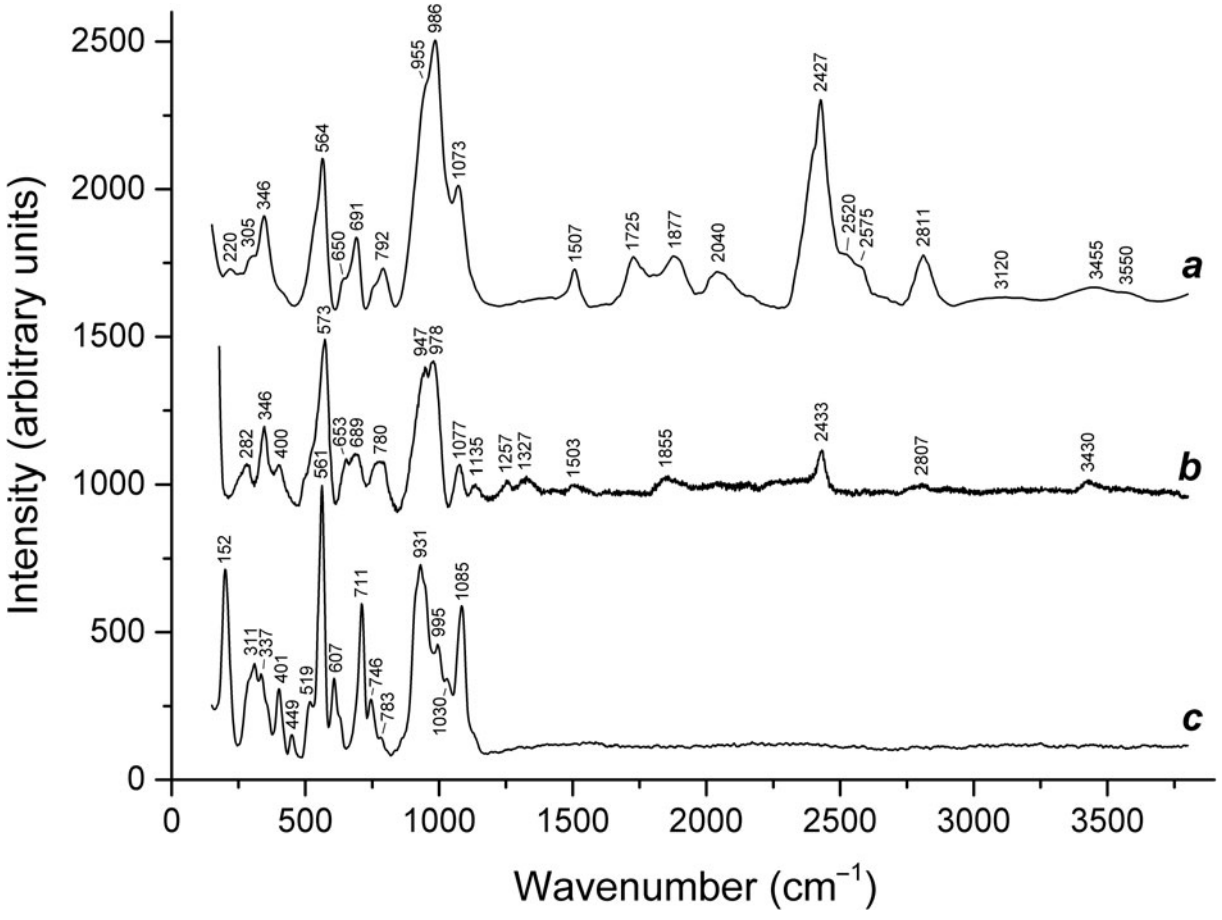

Figure 3. Raman spectra of (a) selsurtite, (b) amableite-(Ce) and (c) eudialyte.

https://doi.org/10.1180/mgm.2024.26 Published online by Cambridge University Press

Table 2. Chemical composition of amableite-(Ce).

Const.	Content (wt.%)	Range	Standard deviation	Standard
Na_2O	14.20	13.75–14.56	0.26	Albite
K_2O	0.41	0.29–0.48	0.07	Orthoclase
CaO	1.89	1.79–1.98	0.06	Wollastonite
MnO*	8.25	8.02–8.50	0.12	Mn
Fe_2O_3	2.40	2.07–2.85	0.21	Fe
La_2O_3	3.10	2.93–3.25	0.10	$LaPO_4$
Ce_2O_3	4.19	3.98–4.34	0.12	$CePO_4$
Pr_2O_3	0.16	0.00–0.25	0.08	$PrPO_4$
Nd_2O_3	0.59	0.50–0.69	0.07	$NdPO_4$
SiO_2	49.41	49.16–49.87	0.25	SiO_2
ZrO_2	11.17	11.09–11.44	0.13	Zr
HfO_2	0.24	0.18–0.29	0.04	Hf
TiO_2	0.68	0.54–0.81	0.08	Ti
Nb_2O_5	1.54	1.30–1.67	0.12	Nb
Cl	0.26	0.21–0.30	0.03	NaCl
H_2O**	1.70			
–O≡Cl	–0.06			
Total	100.13			

*Bivalent state of Mn and trivalent state of Fe are in agreement with the IR spectrum (see above) and structural data. In addition, Mn^{3+} is a very strong purple chromophore whereas amableite-(Ce) is yellow.
**The content of H_2O was determined by means of a modified Penfield method.

the yellow colour of amableite-(Ce) indicates the absence of Fe^{2+} at the *M*2 site. The trivalent state of iron is also in agreement with a superior Gladstone–Dale compatibility index $CI = 1-(K_p/K_c) = -0.014$ (Mandarino, 1981). In comparison, with Fe^{2+}, the CI would be –0.026.

The bulk empirical formula of amableite-(Ce) is $H_{5.76}Na_{14.00}K_{0.27}Ca_{1.03}Ce_{0.78}La_{0.58}Nd_{0.11}Pr_{0.03}Mn_{3.55}Fe_{0.92}Ti_{0.26}Zr_{2.77}Hf_{0.035}Nb_{0.35}Si_{25.12}Cl_{0.22}O_{75.36}$. Based on the structural data (see below), it can be written as: $(Na_{12.93}K_{0.27}Ce_{0.06})_{\Sigma 13.26}[(Mn_{2.49}Ce_{0.30}Ca_{0.21})_{\Sigma 3.00}(Ce_{1.14}Na_{1.04}Ca_{0.82})_{\Sigma 3.00}](Mn_{1.05}Fe_{0.90}\square_{1.05})_{\Sigma 3.00}(Zr_{2.85}Ti_{0.12}Hf_{0.03})_{\Sigma 3.00}(\square_{0.40}Nb_{0.36}Si_{0.24})_{\Sigma 1.00}(Si_{0.88}\square_{0.12})_{\Sigma 1.00}[Si_{24}(O_{70.44}(OH)_{1.56})_{\Sigma 72.00}]\ [(OH)_{2.20}(H_2O)_{1.27}]_{\Sigma 3.47}Cl_{0.22}$.

The simplified formula is $(Na,H,K,Ce)_{15}[(Ce,Na,Ca)_3(Mn,Ce,Ca)_3](Mn,Fe,\square)_3(Zr,Ti)_3(\square,Nb,Si)(Si,\square)Si_{24}(O,OH)_{72}](OH,H_2O,O)_3$, and the ideal formula is $Na_{15}[(Ce_{1.5}Na_{1.5})Mn_3]Mn_2Zr_3\square Si[Si_{24}O_{69}(OH)_3](OH)_2{\cdot}H_2O$.

X-ray diffraction and crystal structure

Powder X-ray diffraction data for amableite-(Ce) are given in Table 3. The unit-cell parameters refined from the powder data are: $a = 14.140(3)$ Å, $c = 30.37(1)$ Å and $V = 5258(4)$ Å^3. The crystal structure of amableite-(Ce) (Figs 4 and 5) was refined on the

Table 3. Powder X-ray diffraction data (*d* in Å) of amableite-(Ce).

I_{obs} (%)	d_{obs} (Å)	I_{calc} (%)*	d_{calc} (Å)**	*h k l*	I_{obs} (%)	d_{obs} (Å)	I_{calc} (%)*	d_{calc} (Å)**	*h k l*
51	**11.34**	**57**	**11.353**	**101**	8	2.112	7	2.112	514
11	10.11	5	10.126	003	6	2.095	4	2.095	$\bar{1}59$
13	9.53	19	9.531	012	8	2.062	2, 5, 2	2.067, 2.062, 2.058	155, $\bar{3}$.5.10, 2.2.12
76	**7.06**	**89**	**7.067**	**110**	4	2.043	1, 2	2.045, 2.041	2.0.14, 247
20	6.45	29	6.453	104	5	2.009	5	2.008	431
32	6.00	21	6.000	021	5	2.001	3	2.000	603
27	5.67	24	5.677	202	11	1.975	11, 2	1.976, 1.969	428, $\bar{2}$.5.11
13	5.44	16	5.442	015	5	1.962	2, 1, 1	1.965, 1.961, 1.960	$\bar{1}$.3.14, $\bar{5}$67, 520
2	5.07	2	5.063	006	4	1.945	2, 2	1.947, 1.945	1.1.15, $\bar{4}$74
4	4.422	2	4.426	$\bar{1}32$	5	1.930	4, 2, 1	1.932, 1.925, 1.924	$\bar{3}$69, 1.3.13, $\bar{2}$73
63	**4.312**	**64**	**4.312**	**205**	2	1.909	1, 1	1.910, 1.906	$\bar{3}$75, 0.5.10
22	4.100	16, 6, 7	4.116, 4.090, 4.080	116, 107, 300	7	1.892	7	1.892	606
26	3.951	25	3.951	214	3	1.863	4	1.863	$\bar{1}$71
38	**3.783**	**36**	**3.784**	**033**	3	1.854	3	1.853	612
8	3.678	6	3.681	125	7	1.837	3, 5	1.840, 1.837	$\bar{2}$.6.10, 4.1.12
6	3.627	7	3.627	018	9	1.829	8, 3	1.829, 1.826	256, 437
43	3.538	33, 11	3.540, 3.534	027, 220	2	1.813	1, 1	1.813, 1.813	0.2.16, $\bar{1}$74
31	3.373	23	3.374	$\bar{1}41$	10	1.781	1, 6	1.784, 1.781	615, 5.1.10
19	3.326	12, 10	3.336, 3.313	223, 312	24	1.769	10, 10, 18	1.773, 1.770, 1.767	$\bar{4}$.6.11, 0.4.14, 440
20	3.224	19	3.227	208	6	1.747	1, 6	1.746, 1.746	069, 701
30	3.168	9, 22	3.177, 3.165	036, $\bar{2}$37	2	1.726	2	1.725	$\bar{3}$.6.12
21	3.044	19, 1	3.046, 3.045	119, 401	5	1.716	5, 2	1.717, 1.715	$\bar{2}$.5.14, 2.0.17
13	2.998	8	3.000	042	3	1.696	4	1.695	621
84	**2.963**	**80**	**2.964**	**$\bar{3}$45**	6	1.688	1, 7	1.688, 1.687	0.0.18, $\bar{2}$82
14	2.898	12	2.898	226	9	1.668	12	1.668	446
100	**2.837**	**100**	**2.838**	**404**	5	1.643	5, 3	1.644, 1.642	2.4.13, 1.1.18
3	2.796	2	2.796	$\bar{3}$51	8	1.637	9	1.635	265
5	2.760	2	2.761	$\bar{2}$52	10	1.613	3, 13	1.614, 1.613	1.4.15, 4.0.16
10	2.721	11	2.721	0.2.10	2	1.602	3	1.601	$\bar{7}$83
22	2.674	20, 6	2.674, 2.671	137, 140	5	1.590	4	1.590	$\bar{1}$.7.10
19	2.633	19	2.634	$\bar{3}$54	7	1.581	1, 1, 7	1.583, 1.581, 1.581	$\bar{4}$.6.14, 3.1.17, 627
17	2.600	26	2.601	039	5	1.573	7	1.573	3.2.16
9	2.532	8, 2	2.536, 2.531	0.0.12, $\bar{3}$48	2	1.559	1, 1	1.560, 1.559	0.3.18, 452
14	2.441	8, 9	2.441, 2.440	229, 051	4	1.550	3	1.550	2.5.12
11	2.382	11	2.383	048	7	1.544	6	1.544	1.5.14
8	2.362	6	2.362	$\bar{4}$56	6	1.524	4, 1, 1, 4	1.525, 1.525, 1.523, 1.522	4.3.13, $\bar{6}$93, 2.2.18, 802
11	2.306	13	2.307	$\bar{2}$61	2	1.500	2, 1	1.500, 1.500	0.5.16, 084
5	2.260	2, 3	2.264, 2.258	$\bar{1}$.4.10, $\bar{2}$58	7	1.478	2, 8	1.482, 1.477	6.2.10, 0.7.11
3	2.193	1	2.193	$\bar{5}$61	2	1.468	3, 1	1.468, 1.467	2.4.16, $\bar{2}$94
8	2.176	5	2.176	$\bar{1}$62	4	1.446	1, 1, 3	1.446, 1.446, 1.443	$\bar{1}$.4.19, $\bar{2}$.8.11, $\bar{1}$.3.20
28	2.157	8, 23	2.162, 2.156	$\bar{4}$65, 4.0.10	2	1.439	2	1.437	0.6.15
13	2.140	8, 4, 2	2.142, 2.137, 2.136	$\bar{3}$.4.11, 0.1.14, $\bar{3}$66	3	1.420	3	1.419	808

*For the calculated pattern, only reflections with intensities ≥1 are given. **For the unit-cell parameters calculated from single-crystal data. The strongest lines are given in bold.

https://doi.org/10.1180/mgm.2024.26 Published online by Cambridge University Press

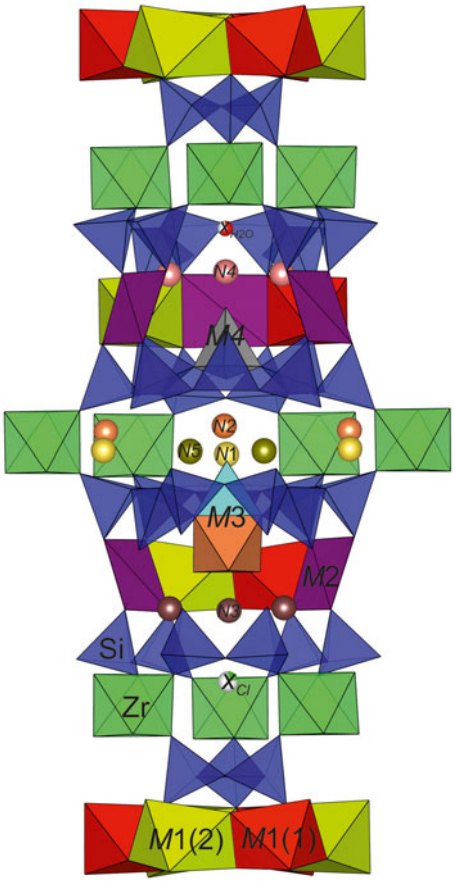

Figure 4. The crystal structure of amableite-(Ce): general view. Drawn with the *DIAMOND* program (Brandenburg and Putz, 2005).

basis of 6462 independent reflections with $I > 2\sigma(I)$. The final refinement cycles converged to $R_1 = 4.23\%$. The atomic coordinates occupancies, site-scattering values and equivalent isotropic parameters are given in Table 4. The anisotropic displacement parameters and selected bond lengths are given in Tables 5 and 6, respectively. See Discussion section for further details. The crystallographic information file (cif) has been deposited *via* the joint Cambridge Crystallographic Data Centre CCDC/FIZ Karlsruhe deposition service https://www.ccdc.cam.ac.uk/structures/ (the deposition number is CSD 2325823) and are also available as Supplementary Material (see below).

Discussion

Crystal structure

Amableite-(Ce) is isostructural with the other 12-layered members of the oneillite subgroup of the eudialyte group with the space group *R*3. Based on the refined site-scattering factors, the crystal chemical formula of amableite-(Ce) can be written as follows ($Z = 3$):

$$^{N1-5}(Na_{12.93}H^{+}_{1.74}K_{0.27}Ce_{0.06})_{\Sigma 15}\ ^{ZrZ}(Zr_{2.85}Ti_{0.12}Hf_{0.03})_{\Sigma 3}$$
$$^{M1(1)}(Mn_{2.49}Ce_{0.30}Ca_{0.21})_{\Sigma 3}\ ^{M1(2)}(Ce_{1.14}Na_{1.04}Ca_{0.82})_{\Sigma 3}$$
$$^{M2}(Mn_{1.05}Fe_{0.90}\square_{1.05})_{\Sigma 3}\ ^{M3}(\square_{0.40}Nb_{0.36}Si_{0.24})_{\Sigma 1}\ ^{M4}(Si_{0.88}\square_{0.12})_{\Sigma 1}$$
$$[^{Si1,2,5-10}Si_{24}O_{70.44}(OH)_{1.56}]\ ^{\varnothing,O25-30}[(OH)_{1.78}O_{1.08}Cl_{0.22}(H_2O)_{0.61}]$$

where $[^{Si1,2,5-10}Si_{24}O_{70.44}(OH)_{1.56}]$ are rings of tetrahedra.

The following combination of structural features of amableite-(Ce) distinguishes it from other eudialyte-group minerals:

(1) Cation ordering within the six-membered ring of octahedra resulting in a lowering of symmetry (Fig. 5). The six-membered ring is formed by $M1(1)O_6$- and $M1(2)O_6$-octahedra with different occupancies. The $M1(1)O_6$-octahedron is predominantly occupied by manganese (2.49 atoms per formula unit), whereas the $M1(2)O_6$-octahedron is predominantly occupied by Na and *REE*, with subordinate Ca.
(2) The predominance of Mn^{2+} at the *M*2 site.
(3) The predominance of vacancies over NbO_6 octahedra and $SiO_3(OH)$ tetrahedra at the *M*3 site.
(4) The predominance of Si at the *M*4 site.

Comparative data for amableite-(Ce) and related eudialyte-group minerals are given in Table 7.

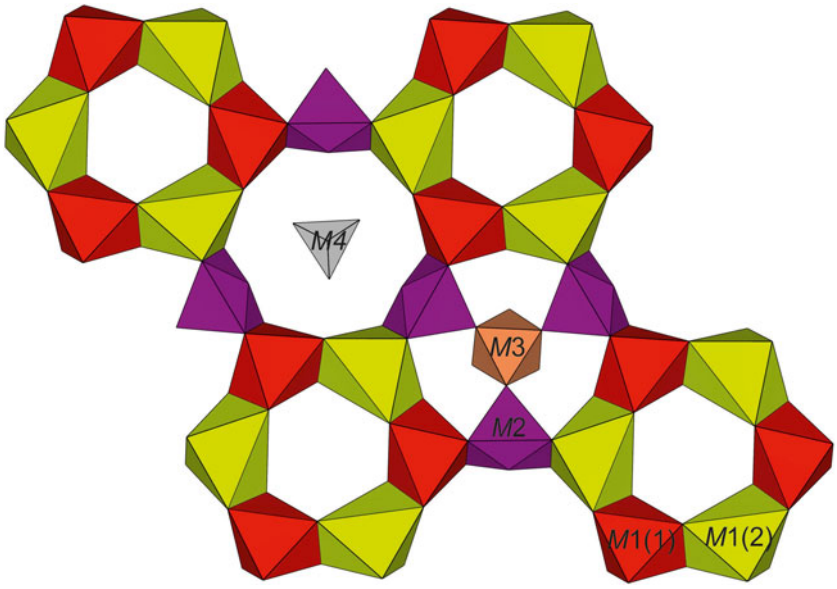

Figure 5. A local arrangement involving 6-membered rings of octahedra in the amableite-(Ce) structure. Drawn with the *DIAMOND* program (Brandenburg and Putz, 2005).

https://doi.org/10.1180/mgm.2024.26 Published online by Cambridge University Press

Table 4. Atomic coordinates, occupancies, site-scattering values and equivalent isotropic displacement parameters (Å^2) for amableite-(Ce).

Site	*x*	*y*	*z*	Occupancy	s.s. calc*	s.s.*	*U*(eq)
Zr*Z*	0.33321(6)	0.16067(5)	0.43713(3)	$Zr_{0.95}Ti_{0.04}Hf_{0.01}$	39.60	40.0	0.0149(1)
***M*1(1)**							
Mn1	0.3938(4)	0.0606(4)	0.6038(1)	$Mn_{0.83}Ce_{0.10}Ca_{0.07}$	27.95	22.25	0.0152(6)
Mn1*A*	0.424(1)	0.090(1)	0.6041(2)			5.50	0.011(2)
***M*1(2)**							
Ce1_2	0.4242(4)	0.3336(1)	0.60390(6)	$Ce_{0.38}Na_{0.35}Ca_{0.27}$	31.29	24.36	0.0171(7)
Na1_2	0.394(2)	0.3316(9)	0.6034(4)			6.50	0.029(3)
***M*2**							
Mn2_1	0.4943(8)	0.4934(8)	0.2705(2)	$Mn_{0.35}\square_{0.35}Fe_{0.30}$	16.55	12.75	0.049(7)
Mn2_2	0.469(2)	0.525(2)	0.2718(9)			2.00	0.021(6)
Mn2_3	0.523(2)	0.473(2)	0.2682(9)			1.63	0.014(7)
Si1	0.3927(1)	0.3814(1)	0.36682(7)	Si	14.0	14.0	0.0172(4)
Si2	0.6079(1)	0.6001(1)	0.36659(7)	Si	14.0	14.0	0.0167(4)
Si5	0.2740(1)	0.3221(1)	0.50743(7)	Si	14.0	14.0	0.0171(4)
Si6	0.2071(1)	0.4149(2)	0.34589(8)	Si	14.0	14.0	0.0211(4)
Si7	0.5263(1)	0.2521(2)	0.52327(8)	Si	14.0	14.0	0.0205(4)
Si8	0.0586(1)	0.3253(1)	0.50773(7)	Si	14.0	14.0	0.0163(4)
Si9	0.5856(2)	0.1928(1)	0.68446(7)	Si	14.0	14.0	0.0199(4)
Si10	0.4597(2)	0.5413(2)	0.52849(8)	Si	14.0	14.0	0.0217(4)
***M*3**							
Nb*M*3	⅓	⅔	0.5585(2)	$\square_{0.40}Nb_{0.36}Si_{0.24}$	17.85	14.35	0.047(2)
Si*M*3	⅓	⅔	0.5152(8)			3.50	0.039(8)
***M*4**							
Si*M*4	⅓	⅔	0.3167(2)	$Si_{0.88}\square_{0.12}$	12.32	10.22	0.030(2)
Si*M*4A	⅓	⅔	0.3594(9)			2.10	0.016(8)
***N*1–*N*5**							
Na*N*1	0.5514(4)	0.4416(4)	0.4499(2)	Na	11.0	11.0	0.052(1)
Na*N*2	0.1169(5)	0.2285(6)	0.4225(2)	Na	11.0	6.60	0.027(1)
Na*N*2A	0.086(2)	0.167(2)	0.4389(6)			4.40	0.11(1)
Na*N*3	0.4612(5)	0.2283(4)	0.3151(2)	$Na_{0.89}K_{0.09}Ce_{0.02}$	12.66	11.83	0.058(2)
Na*N*3A	0.528(4)	0.263(3)	0.324(2)			1.59	0.06(1)
Na*N*4	0.2034(7)	0.0996(4)	0.5593(4)	$Na_{0.71}H^+_{0.29}$	7.81	7.15	0.031(3)
Na*N*4A	0.187(4)	0.093(4)	0.580(3)			0.66	0.01(2)
Na*N*5	0.268(2)	0.533(1)	0.4492(5)	$Na_{0.71}H^+_{0.29}$	7.81	7.81	0.153(9)
O1	0.2666(6)	0.2903(6)	0.5577(3)	O	8.0	8.0	0.041(2)
O2	0.3932(4)	0.4304(5)	0.4975(2)	O	8.0	8.0	0.029(1)
O3	0.4073(6)	0.3024(6)	0.3996(3)	O	8.0	8.0	0.036(2)
O4	0.4850(4)	0.5067(4)	0.3805(3)	O	8.0	8.0	0.030(1)
O5	0.2609(5)	0.2282(5)	0.4748(3)	O	8.0	8.0	0.033(1)
O6	0.7192(5)	0.2620(5)	0.6810(3)	O	8.0	8.0	0.033(1)
O7	0.3883(7)	0.5991(6)	0.5313(4)	O	8.0	8.0	0.054(2)
O8	0.4009(5)	0.3591(6)	0.3161(2)	O	8.0	8.0	0.035(1)
O9	0.4953(5)	0.5169(5)	0.5750(3)	O	8.0	8.0	0.031(1)
O10	0.2736(5)	0.3716(5)	0.3759(2)	O	8.0	8.0	0.028(1)
O11	0.6884(5)	0.5862(5)	0.3988(3)	O	8.0	8.0	0.035(1)
O12	−0.0223(5)	0.2293(5)	0.4757(3)	O	8.0	8.0	0.031(1)
O13	0.1813(5)	0.3543(5)	0.4939(3)	O	8.0	8.0	0.030(1)
O14	0.1731(6)	0.3575(6)	0.2993(3)	O	8.0	8.0	0.030(1)
O15	0.5959(5)	0.3858(5)	0.5261(3)	O	8.0	8.0	0.033(2)
O16	0.5525(6)	0.1366(6)	0.7315(3)	O	8.0	8.0	0.041(2)
O17	0.4714(6)	0.2217(7)	0.4754(3)	O	8.0	8.0	0.040(2)
O18	0.0510(6)	0.4347(5)	0.4971(2)	O	8.0	8.0	0.033(1)
O19	0.0369(6)	0.2968(6)	0.5591(2)	O	8.0	8.0	0.035(1)
O20	0.5359(6)	0.1122(5)	0.6438(2)	O	8.0	8.0	0.039(1)
O21	0.4452(5)	0.2037(6)	0.5639(2)	O	8.0	8.0	0.039(1)
O22	0.6282(6)	0.5914(5)	0.3148(2)	O	8.0	8.0	0.029(1)
O23	0.1012(5)	0.3849(6)	0.3767(2)	O	8.0	8.0	0.031(1)
O24	0.2787(7)	0.5449(5)	0.3432(4)	O	8.0	8.0	0.059(3)
O,OH,Cl,H_2O							
O25	0	0	0.5028(8)	$(H_2O)_{0.61}$	4.88	4.88	0.050**
O26	⅓	⅔	0.268(1)	$OH_{0.73}$	5.84	5.84	0.12(1)
O27	0.277(2)	0.731(2)	0.6012(7)	$O_{0.36}OH_{0.22}$	4.64	4.72	0.089(9)
Cl28	⅔	⅓	0.407(1)	$Cl_{0.22}$	3.74	3.74	0.050**
O29	⅓	⅔	0.413(1)	$OH_{0.15}$	1.20	1.20	0.050**
O30	⅓	⅔	0.461(1)	$OH_{0.24}$	1.92	1.92	0.050**

*s.s. – site scattering; calc. s.s. – calculated site scattering (electrons per formula unit). ** Fixed parameters.

https://doi.org/10.1180/mgm.2024.26 Published online by Cambridge University Press

Table 5. Anisotropic displacement parameters (Å^2) for amableite-(Ce).

Site	U^{11}	U^{22}	U^{33}	U^{23}	U^{13}	U^{12}
ZrZ	0.0142(2)	0.0157(3)	0.0144(2)	0.0003(2)	0.0007(2)	0.0071(2)
Mn1	0.015(1)	0.015(1)	0.0136(6)	0.001(5)	–0.0011(5)	0.006(1)
Ce1_2	0.020(1)	0.0097(6)	0.0172(6)	–0.0011(3)	–0.0002(5)	0.0038(5)
Na1_2	0.014(5)	0.040(6)	0.032(5)	0.002(3)	–0.003(3)	0.013(4)
Mn2	0.039(5)	0.040(5)	0.018(2)	0.012(2)	–0.011(2)	–0.017(5)
Si1	0.0130(7)	0.0190(8)	0.019(1)	0.0023(7)	–0.0004(6)	0.0076(6)
Si2	0.0203(8)	0.0133(7)	0.016(1)	0.0018(6)	0(7)	0.0083(6)
Si5	0.0127(7)	0.0162(8)	0.019(1)	–0.0024(7)	–0.0005(6)	0.0050(6)
Si6	0.0164(8)	0.0213(9)	0.027(1)	–0.0079(8)	–0.0024(7)	0.0107(7)
Si7	0.0095(7)	0.0279(9)	0.018(1)	–0.0006(7)	0.0015(6)	0.0050(6)
Si8	0.0198(8)	0.0178(8)	0.015(1)	–0.0020(6)	–0.0002(6)	0.0123(6)
Si9	0.0279(9)	0.0088(7)	0.0161(9)	–0.0022(6)	–0.0008(7)	0.0041(6)
Si10	0.0163(8)	0.0161(8)	0.029(1)	0.0049(7)	–0.0029(7)	0.0056(7)
Nb*M3*	0.039(2)	0.039(2)	0.064(4)	0	0	0.019(1)
Si*M3*	0.035(8)	0.035(8)	0.05(2)	0	0	0.017(4)
Si*M4*	0.023(2)	0.023(2)	0.043(4)	0	0	0.012(1)
Si*M4A*	0.008(7)	0.008(7)	0.03(2)	0	0	0.004(4)
Na*N1*	0.042(2)	0.055(3)	0.039(3)	0.012(2)	–0.013(2)	0.009(2)
Na*N2*	0.021(2)	0.037(3)	0.020(3)	–0.006(2)	–0.006(2)	0.012(2)
Na*N2A*	0.10(1)	0.24(3)	0.07(1)	–0.10(2)	–0.06(1)	0.14(2)
Na*N3*	0.079(4)	0.038(2)	0.071(4)	–0.019(2)	–0.034(3)	0.041(2)
Na*N4*	0.052(4)	0.013(2)	0.037(6)	–0.011(2)	–0.022(4)	0.024(2)
Na*N5*	0.23(2)	0.12(1)	0.12(1)	–0.020(8)	–0.02(1)	0.09(1)
O1	0.037(3)	0.041(4)	0.022(4)	0.002(3)	–0.004(3)	0.004(3)
O2	0.015(2)	0.022(2)	0.040(4)	–0.006(2)	0(2)	0.0007(2)
O3	0.034(3)	0.034(3)	0.043(4)	0.022(3)	0.010(3)	0.020(3)
O4	0.020(2)	0.019(2)	0.044(5)	–0.002(2)	0.002(2)	0.004(2)
O5	0.035(3)	0.027(3)	0.037(4)	–0.011(3)	0.002(3)	0.017(3)
O6	0.023(2)	0.024(2)	0.058(4)	0.005(2)	0.006(2)	0.016(2)
O7	0.048(4)	0.040(4)	0.089(7)	–0.003(4)	–0.008(4)	0.034(4)
O8	0.034(3)	0.057(4)	0.022(3)	–0.010(3)	–0.005(2)	0.028(3)
O9	0.037(3)	0.031(3)	0.023(4)	0.007(2)	-0.001(2)	0.015(3)
O10	0.018(2)	0.029(3)	0.037(4)	0(2)	0.002(2)	0.013(2)
O11	0.029(3)	0.033(3)	0.043(4)	–0.005(3)	–0.019(3)	0.016(3)
O12	0.031(3)	0.025(3)	0.036(4)	–0.008(3)	–0.010(3)	0.012(2)
O13	0.022(2)	0.032(3)	0.039(4)	0.002(2)	0.002(2)	0.016(2)
O14	0.041(3)	0.031(3)	0.019(3)	–0.006(3)	0(2)	0.019(3)
O15	0.023(2)	0.019(2)	0.064(5)	–0.006(3)	–0.003(3)	0.015(2)
O16	0.047(4)	0.034(3)	0.029(4)	0.010(3)	0.005(3)	0.010(3)
O17	0.028(3)	0.060(4)	0.021(3)	–0.010(3)	–0.007(2)	0.015(3)
O18	0.059(4)	0.029(3)	0.028(3)	0.001(2)	0.003(3)	0.034(3)
O19	0.060(4)	0.034(3)	0.020(3)	0.002(2)	0.006(3)	0.030(3)
O20	0.052(4)	0.033(3)	0.031(3)	–0.019(3)	–0.011(3)	0.022(3)
O21	0.035(3)	0.051(4)	0.026(3)	0.014(3)	0.018(3)	0.017(3)
O22	0.047(3)	0.027(3)	0.019(3)	0.006(2)	0.007(2)	0.022(3)
O23	0.026(3)	0.053(4)	0.025(3)	–0.003(3)	–0.005(2)	0.028(3)
O24	0.045(4)	0.013(3)	0.115(9)	0.001(4)	–0.007(5)	0.011(3)

Raman spectroscopy of hydronium and hydrated proton complexes

Numerous *ab initio* quantum-chemical calculations of hydronium and other hydrated proton complexes, including Zundel ($H_5O_2^+$) and Eigen ($H_3O^+ \cdot 3H_2O$) cations have shown that these clusters are characterised by variable configurations and strong hydrogen bonds with the O···O distances in the range of 2.38–2.8 Å (Vyas, 1978; Komatsuzaki and Ohmine, 1994; Corongiu, 1995; Kim *et al.*, 2002; Sobolewski and Domcke, 2002a, 2002b; Asmis *et al.*, 2003; Christie, 2004; Headrick *et al.*, 2004; Laria *et al.*, 2004; Asthagiri *et al.*, 2005; Ortega *et al*, 2005; Paddison and Elliott, 2005; Vener and Librovich, 2009; Biswas *et al.*, 2017; Carpenter, 2020). Calculated wavenumbers of vibrational modes corresponding to the hydrated proton complexes are in the range of 1070–3000 cm^{-1}.

There is a negative correlation between the frequency of O–H stretching vibrations and O···O distance between the O atom of OH group and the O atom – acceptor of the hydrogen bond (McClellan and Pimentel, 1960; see Fig. 6). This correlation is nearly linear in the range of the O···O distances from 2.4 to 2.8 Å and significantly deviates from the linearity for weaker hydrogen bonds.

The following empirical correlations between O–H stretching frequencies in IR spectra of minerals and O···O and H···O distances (obtained from structural data) were established by E. Libowitzky (1999):

$$\nu(\mathrm{cm}^{-1}) = 3592 - 304 \cdot 10^9 \cdot \exp[-d(\mathrm{O}\cdots\mathrm{O})/0.1321] \quad (1)$$

$$\nu(\mathrm{cm}^{-1}) = 3632 - 1.79 \cdot 10^6 \cdot \exp[-d(\mathrm{H}\cdots\mathrm{O})/0.2146] \quad (2)$$

A similar correlation was obtained by Novak (1974).

In reality, equations 1 and 2 are a very rough approximation and have restricted applicability. In particular, above 3500 cm^{-1} substantial deviations from correlations 1 and 2 are common because O–H stretching frequencies depend not only on O···O and H···O distances, but also on the nature of cations coordinating O–H groups and H_2O molecules, as well as on the O–H···O angle, and the influence of these factors becomes most evident in the case of weak hydrogen bonds. The equations 1 and 2 predict that maximum possible values of O–H stretching frequencies for minerals are 3592 and 3632 cm^{-1}, respectively, but in many minerals including for magnesium serpentines, brucite, kaolinite, amphiboles etc. observed frequencies are much higher and can exceed 3700 cm^{-1}. However, these correlations can be used for semiquantitative estimations, at least for relatively strong hydrogen bonds.

According to the equation (1), the Raman bands of amableite-(Ce) observed at 1815, 2433 and 2807 cm^{-1} correspond to the O···O distances of 2.51, 2.56 and 2.61 Å, respectively which is quite close to the distances of 2.50, 2.58 and 2.59 Å for O7···O30, O7···O27 and O24···O29 in strong hydrogen bonds O–H···O in amableite-(Ce).

Implications

Minerals belonging to the eudialyte group are considered as potential sources of *REE*, Zr, Hf, Nb and Ta for industrial use (Lebedev, 2003; Lebedev *et al.*, 2003; Zakharov *et al.*, 2011; Friedrich *et al.*, 2016; Davis *et al.*, 2017; Ma *et al.*, 2019). Almost all the samples of EGMs studied contain detectable amounts of rare-earth elements (Rastsvetaeva *et al.*, 2012). Samples of EGMs from peralkaline pegmatites are characterised by the highest contents of these elements (typically, from 2 to 8 wt.% of REE_2O_3). Amableite-(Ce) is the third EGM after zirsilite-(Ce), $(Na,\square)_{12}(Ce,Na)_3Ca_6Mn_3Zr_3Nb(Si_{25}O_{73})(OH)_3(CO_3)\cdot H_2O$ (Khomyakov *et al.*, 2003) and johnsenite-(Ce), $Na_{12}(Ce,La,Sr,Ca)_3Ca_6Mn_3Zr_3W(Si_{25}O_{73})(OH,Cl)_2(CO_3)$ (Grice and Gault, 2006) containing *REE* as a species-defining component.

As a rule, *REE*-rich EGMs are enriched in Mn whereas *REE*-poor EGMs are enriched in Fe. This regularity may have a crystal-chemical origin and correspond to the situations where relatively small (Fe- and Ca-centred) or larger (Mn^{2+} and *REE*-centred) *M*2- and *M*1-octahedra share common edges. However, geochemical factors may also play a significant role.

https://doi.org/10.1180/mgm.2024.26 Published online by Cambridge University Press

Table 6. Selected bond lengths (*d* in Å) in amableite-(Ce).

Zr*Z*–O3	2.076(7)	Na1_2–O1	2.11(2)	Si1–O3	1.585(7)	Si9–O6	1.636(6)	Na*N*1–O2	2.601(9)	Na*N*3A–O3	3.07(4)
Zr*Z*–O5	2.059(7)	Na1_2–O8	2.13(2)	Si1–O4	1.643(6)	Si9–O6	1.638(6)	Na*N*1–O3	2.520(10)	Na*N*3A –O8	2.75(4)
Zr*Z*–O11	2.068(6)	Na1_2–O9	2.431(13)	Si1–O8	1.590(8)	Si9–O16	1.589(6)	Na*N*1–O4	2.652(9)	Na*N*3A –O11	3.04(4)
Zr*Z*–O12	2.067(7)	Na1_2–O14	2.408(13)	Si1–O10	1.641(6)	Si9–O20	1.588(6)	Na*N*1–O11	2.526(9)	Na*N*3A –O22	2.78(4)
Zr*Z*–O16	2.051(7)	Na1_2–O20	2.61(2)	<Si1–O>	1.615	<Si9–O>	1.612	Na*N*1–O15	2.620(9)	Na*N*3A –O27	2.38(4)
Zr*Z*–O17	2.056(7)	Na1_2–O21	2.56(2)					Na*N*1–O17	2.833(10)	Na*N*3A –O27	2.30(4)
<Zr*Z*–O>	2.063	<Na1_2–O>	2.377	Si2–O4	1.628(6)	Si10–O2	1.659(6)	Na*N*1–O17	2.559(9)	Na*N*3A –Cl28	3.03(5)
				Si2–O11	1.588(7)	Si10–O7	1.586(8)	Na*N*1–O18	2.775(10)	<Na*N*3A–O,OH,Cl>	2.76
Mn1–O9	2.274(7)	Mn2_1–O1	2.216(10)	Si2–O22	1.613(7)	Si10–O9	1.595(8)	Na*N*1–Cl28	3.036(12)		
Mn1–O14	2.292(7)	Mn2_1–O8	2.181(9)	Si2–O23	1.623(6)	Si10–O18	1.637(7)	<Na*N*1–O,Cl>	2.680	Na*N*4–O1	2.380(9)
Mn1–O19	2.171(9)	Mn2_1–O19	2.195(9)	<Si2–O>	1.613	<Si10–O>	1.620			Na*N*4–O5	3.013(14)
Mn1–O20	2.140(8)	Mn2_1–O22	2.165(8)					Na*N*2–O5	2.584(11)	Na*N*4–O12	2.975(14)
Mn1–O21	2.149(8)	Mn2_1–O27	2.61(3)	Si5–O1	1.581(8)	Si*M3*–O7	1.580(11)	Na*N*2–O6	2.610(11)	Na*N*4–O14	2.578(11)
Mn1–O22	2.183(8)	<Mn2_1–O,OH>	2.273	Si5–O2	1.640(6)	Si*M3*–O7	1.580(11)	Na*N*2–O10	2.554(9)	Na*N*4–O19	2.428(8)
<Mn1–O>	2.202			Si5–O5	1.592(7)	Si*M3*–O7	1.580(11)	Na*N*2–O12	2.550(11)	Na*N*4–O21	2.972(10)
		Mn2_2–O1	2.20(2)	Si5–O13	1.640(6)	Si*M3*–O30	1.63(3)	Na*N*2–O13	2.660(11)	Na*N*4–O25	3.024(14)
Mn1*A*–O9	2.301(10)	Mn2_2–O8	2.42(3)	<Si5–O>	1.613	<Si*M3*–O,OH>	1.592	Na*N*2–O16	2.559(11)	Na*N*4–O26	2.81(2)
Mn1*A*–O14	2.327(10)	Mn2_2–O19	2.16(3)					Na*N*2–O16	2.898(11)	<Na*N*4–O,OH,H_2O>	2.773
Mn1*A*–O19	2.505(18)	Mn2_2–O22	2.35(3)	Si6–O10	1.632(8)	Si*M4*–O24	1.697(9)	Na*N*2–O23	2.713(10)		
Mn1*A*–O20	1.891(14)	<Mn2_2–O>	2.28	Si6–O14	1.582(10)	Si*M4*–O24	1.697(9)	<Na*N*2–O>	2.641	Na*N*4A–O1	2.51(5)
Mn1*A*–O21	1.919(13)			Si6–O23	1.632(8)	Si*M4*–O24	1.697(9)			Na*N*4A–O14	2.20(7)
Mn1*A*–O22	2.508(17)	Mn2_3–O1	2.44(4)	Si6–O24	1.596(7)	Si*M4*–O26	1.46(4)	Na*N*2A–O5	2.436(17)	Na*N*4A–O19	2.59(5)
<Mn1*A*–O>	2.242	Mn2_3–O8	2.22(2)	<Si6–O>	1.610	<Si*M4*–O,OH>	1.638	Na*N*2A–O6	2.821(17)	Na*N*4A–O24	3.06(9)
		Mn2_3–O19	2.32(2)					Na*N*2A–O12	2.389(16)	Na*N*4A–O26	2.39(5)
Ce1_2–O1	2.438(9)	Mn2_3–O22	2.13(3)	Si7–O15	1.639(6)	Si*M4A*–O24	1.572(11)	Na*N*2A–O13	2.84(2)	<Na*N*4A–O,OH>	2.55
Ce1_2–O8	2.438(8)	Mn2_3–O27	2.00(4)	Si7–O15	1.625(6)	Si*M4A* –O24	1.572(11)	Na*N*2A–O16	2.442(17)		
Ce1_2–O9	2.427(7)	<Mn2_3–O,OH>	2.19	Si7–O17	1.603(7)	Si*M4A*–O24	1.572(11)	Na*N*2A–O16	2.697(16)	Na*N*5–O2	3.16(2)
Ce1_2–O14	2.445(7)			Si7–O21	1.588(6)	Si*M4A*–O29	1.63(3)	Na*N*2A–O25	2.82(4)	Na*N*5–O7	2.898(19)
Ce1_2–O20	2.350(8)	Nb*M3*–O7	1.715(9)	<Si7–O>	1.614	<Si*M4A*–O,OH>	1.587	<Na2A–O,H_2O>	2.635	Na*N*5–O7	3.00(2)
Ce1_2–O21	2.340(8)	Nb*M3*–O7	1.715(9)							Na*N*5–O13	2.579(19)
<Ce1_2–O>	2.406	Nb*M3*–O7	1.715(9)	Si8–O12	1.595(7)			Na*N*3–O3	3.012(10)	Na*N*5–O18	3.03(2)
		Nb*M3*–O27	1.96(2)	Si8–O13	1.625(6)			Na*N*3–O8	2.392(8)	Na*N*5–O23	3.141(18)
		Nb*M3*–O27	1.96(2)	Si8–O18	1.635(6)			Na*N*3–O9	2.581(10)	Na*N*5–O29	1.97(3)
		Nb*M3*–O27	1.96(2)	Si8–O19	1.603(8)			Na*N*3–O11	2.982(10)	Na*N*5–O30	1.673(17)
		<Nb*M3*–O>	1.837	<Si8–O>	1.614			Na*N*3–O20	2.953(9)	<Na*N*5–O,OH>	2.681
								Na*N*3–O22	2.423(8)		
								Na*N*3–O27	2.55(2)		
								Na*N*3–O27	2.68(2)		
								<Na*N*3–O,OH>	2.697		

Table 7. Comparative data for amableite-(Ce) and related eudialyte-group minerals with *R*3 symmetry.

Mineral	Amableite-(Ce)	Voronkovite	Oneillite	Raslakite	Sergevanite
Idealised formula	$Na_{15}[(Ce_{1.5}Na_{1.5})Mn_3]$ $Mn_2Zr_3\square Si[Si_{24}O_{69}$ $(OH)_3](OH)_2{\cdot}H_2O$	$Na_{15}[(Na,Ca)_3Mn_3]$ $Fe_3^{2+}Zr_3Si_2(Si_{24}O_{72})$ $(OH,O)_4Cl{\cdot}H_2O$	$Na_{15}[Ca_3Mn_3]Fe_3Zr_3$ $[SiNb](Si_{24}O_{72})$ $(O,OH,H_2O)_4Cl_2$	$Na_{15}[Ca_3Fe_3](Na,Zr)_3$ $Zr_3[(Si,Nb)Si](Si_{24}O_{72})$ $(OH,H_2O,O)_4Cl$	$Na_{15}[Ca_3Mn_3](Na_2Fe^{2+})Zr_3$ $[Si(Si,Ti)][Si_{24}O_{72}]$ $(OH,H_2O,SO_4)_5$
a (Å)	14.1340	14.205	14.2084	14.229	14.2179
c (Å)	30.3780	30.265	29.959	30.019	30.3492
V (Å^3)	5255.6	5289	5237.8	5263.5	5313.11
Strongest lines of the powder X-ray diffraction pattern: *d*, Å (*I*, %)	11.34 (51)	4.316(85)	11.348 (44)	4.311 (66)	7.12 (70)
	7.06 (76)	3.536(41)	6.021 (36)	4.095 (37)	5.711 (43)
	4.312 (63)	3.221(43)	4.291 (37)	3.209 (58)	4.321 (72)
	3.783 (38)	3.039(41)	3.389 (43)	3.023 (40)	3.551 (39)
	3.538 (43)	2.970(100)	3.150 (35)	2.974 (86)	3.398 (39)
	2.963 (84)	2.848(84)	2.964 (100)	2.853 (100)	2.978 (95)
	2.837 (100)		2.844 (89)		2.855 (100)
Optical data	Biaxial (+)	Uniaxial (+)	Uniaxial (–)	Uniaxial (+)	Uniaxial (+)
	$\alpha \approx \beta = 1.603$	$\omega = 1.610$	$\omega = 1.6450$	$\omega = 1.608$	$\omega = 1.604$
	$\gamma = 1.608$, $2V = 20°$	$\varepsilon = 1.619$	$\varepsilon = 1.6406$	$\varepsilon = 1.611$	$\varepsilon = 1.607$
Density (g·cm^{-3})	2.89 (meas.)	2.97 (meas.)	3.20 (meas.)	2.95 (meas.)	2.90 (meas.)
	2.899 (calc.)	2.95 (calc.)	3.22 (calc.)	2.945 (calc.)	2.906 (calc.)
Dominant components at the key sites					
*M*1(1)	Ce+Na	Na	Ca	Ca	Ca
M1(2)	Mn^{2+}	Mn^{2+}	Mn^{2+}	Fe^{2+}	Mn^{2+}
*M*2	Mn^{2+}	Fe^{2+}	Fe^{2+}	Na	Na
*M*3	□	Si	Nb	Si	Si
*M*4	Si	Si	Si	Si	Si
References	This study	Khomyakov *et al*. (2009)	Johnsen *et al*. (1999)	Chukanov *et al*. (2003)	Chukanov *et al*. (2020)

https://doi.org/10.1180/mgm.2024.26 Published online by Cambridge University Press

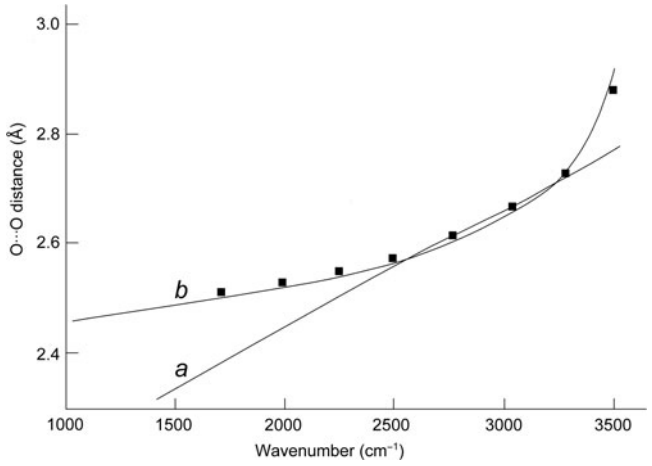

Figure 6. The correlations between wavenumbers of O–H stretching vibrations and O···O distances for hydrogen bonds in crystals drawn using data by McClellan and Pimentel (1960) (curve *a*), Libowitzky (1999) (curve *b*), and Novak (1974) (squares).

Acknowledgements. The authors are grateful to Dr. Henrik Friis and anonymous reviewers for useful comments. A part of this work, including chemical analyses, infrared spectroscopy, interpretation of the Raman spectra and identification of associated minerals was carried-out in accordance with the state task of Russian Federation, registration number 124013100858-3. The authors thank the X-ray Diffraction Centre of Saint-Petersburg State University for instrumental and computational resources. Structure determination was done at the Center for X-Ray Diffraction Studies of the Research Park of St. Petersburg State University within the project AAAA-A19-119091190094-6.

Conflict of interest. The authors declare no conflict of interest.

Supplementary material. Crystallographic information files have been deposited at https://www.ccdc.cam.ac.uk/structures/ (the deposition number is CSD 2325823). In addition they can be found with this article at https://doi.org/10.1180/mgm.2024.26

References

Asmis K.R., Pivonka N.L., Santambrogio G., Brümmer M., Kaposta C., Neumark D.M. and Wöste L. (2003) The gasphase infrared spectrum of the protonated water dimer. *Science*, **299**, 1375–1381.

Asthagiri D., Pratt L.R. and Kress J.D. (2005) *Ab initio* molecular dynamics and quasichemical study of $H^+(aq)$. *Proceedings of the National Academy of Sciences of the United States of America*, **102**, 6704–6708. www.pnas.org_cgi_doi_10.1073_pnas.0408071102

Biswas R., Carpenter W., Fournier J.A., Voth G.A. and Tokmakoff A. (2017) IR spectral assignments for the hydrated excess proton in liquid water. *Journal of Chemical Physics*, **146**, paper 154507. https://doi.org/10.1063/1.4980121

Brandenburg K. and Putz H. (2005) *DIAMOND Version 3*. Crystal Impact GbR. Bonn, Germany.

Britvin S.N., Dolivo-Dobrovolsky D.V. and Krzhizhanovskaya M.G. (2017) Software for processing the X-ray powder diffraction data obtained from the curved image plate detector of Rigaku RAXIS Rapid II diffractometer. *Zapiski Rossiiskogo Mineralogicheskogo Obshchestva* (*Proc. Russ. Mineral. Soc.*), **146**, 104–107.

Carpenter W.B. (2020) *Aqueous Proton Structures and Dynamics Observed With Nonlinear Infrared Spectroscopy*. Ph. D. dissertation, the University of Chicago, 346 pp.

Christie R.A. (2004) *Theoretical Studies of Hydrogen-Bonded Clusters*. Ph.D. Thesis, University of Pittsburgh, 135 pp.

Chukanov N.V., Pekov I.V., Zadov A.E., Korovushkin V.V., Ekimenkova I.A. and Rastsvetaeva R.K. (2003) Ikranite, $(Na,H_3O)_{15}(Ca,Mn,REE)_6Fe^{3+}_2Zr^{3}(□,Zr)(□,Si)Si_{24}O_{66}(O,OH)_6Cl{\cdot}nH_2O$, and raslakite, $Na_{15}Ca_3Fe_3(Na,Zr)_3Zr_3(Si,Nb)(Si_{25}O_{73})(OH,H_2O)_3(Cl,OH)$, new eudialyte-group minerals from the Lovizero massif. *Zapiski Rossiiskogo Mineralogicheskogo Obshchestva* (*Proceedings of the Russian Mineralogical Society*), **132**, 22–33 [in Russian].

Chukanov N.V., Aksenov S.M., Pekov I.V., Belakovskiy D.I., Vozchikova S.A. and Britvin S.N. (2020) Sergevanite, $Na_{15}(Ca_3Mn_3)(Na_2Fe)Zr_3Si_{26}O_{72}(OH)_3{\cdot}H_2O$, a new eudialyte-group mineral from the Lovozero alkaline massif, Kola Peninsula. *The Canadian Mineralogist*, **58**, 421–436, https://doi.org/10.3749/canmin.2000006.

Chukanov N.V., Vigasina M.F., Rastsvetaeva R.K., Aksenov S.M., Mikhailova Ju.A. and Pekov I.V. (2022) The evidence of hydrated proton in eudialyte-group minerals based on Raman spectroscopy data. *Journal of Raman Spectroscopy*, **53**, 1188–1203, https://doi.org/10.1002/jrs.6343.

Chukanov N.V., Aksenov S.M., Kazheva O.N., Pekov I.V., Varlamov D.A., Vigasina M.F., Belakovskiy D.I., Vozchikova S.A. and Britvin S.N. (2023) Selsurtite, $(H_3O)_{12}Na_3(Ca_3Mn_3)(Na_2Fe)Zr_3□Si[Si_{24}O_{69}(OH)_3]$ (OH)Cl·H_2O, a new eudialyte-group mineral from the Lovozero alkaline massif, Kola Peninsula. *Mineralogical Magazine*, **87**, 241–251, https://doi.org/10.1180/mgm.2022.136.

Chukanov N.V., Zolotarev A.A., Schäfer C., Varlamov D.A., Pekov I.V., Vigasina M.F., Belakovskiy D.I., Aksenov S.M., Vozchikova S.A. and Britvin S.N. (2024) Amableite-(Ce), IMA 2023-075. CNMNC Newsletter 77. *Mineralogical Magazine*, **88**, 203–209, https://doi.org/10.1180/mgm.2024.5.

Corongiu G., Kelterbaum R. and Kochanski E. (1995) Theoretical studies of $H^+(H_2O)_5$. *Journal of Physical Chemistry*, **99**, 8038–8044, https://doi.org/10.1021/J100020A029.

CrysAlisPro (2015) *CrysAlisPro Software System, version 1.171.39.44*. Rigaku Oxford Diffraction: Oxford, UK.

Davis P., Stopic S., Balomenos E., Panias D., Paspaliaris I. and Friedrich B. (2017) Leaching of rare earth elements from eudialyte concentrate by suppressing silica gel formation. *Minerals Engineering*, **108**, 115–122.

Dolomanov O.V., Bourhis L.J., Gildea R.J., Howard J.A.K. and Puschmann H. (2009) OLEX2: a complete structure solution, refinement and analysis program. *Journal of Applied Crystallography*, **42**, 339–341.

Friedrich B., Hanebuth M., Kruse S., Tremel A. and Vossenkaul D. (2016) Method for opening a eudialyte mineral. Patent number EP2995692 A1.

Grice J.D. and Gault R.A. (2006) Johnsenite-(Ce): a new member of the eudialyte group from Mont Saint-Hilaire, Quebec, Canada. *The Canadian Mineralogist*, **44**, 105–115.

Headrick J.M., Bopp J.C. and Johnson M.A. (2004) Predissociation spectroscopy of the argon-solvated $H_5O_2^+$ "Zundel" cation in the 1000–1900 cm^{-1} region. *Journal of Chemical Physics*, **121**, 11523–11526.

Horváth L., Pfenninger Horváthm E., Gault R.A. and Tarasoff P. (1998) Mineralogy of the Saint Amable sill, Varennes and Saint Amable, Québec, Canada. *Mineralogical Record*, **29**, 83–118.

Johnsen O., Grice J.D. and Gault R.A. (1999) Oneillite: a new Ca-deficient and *REE*-rich member of the eudialyte group from Mont Saint-Hilaire, Québec, Canada. *The Canadian Mineralogist*, **37**, 1295–1301.

Johnsen O., Ferraris G., Gault R.A., Grice J.D., Kampf A.R. and Pekov I.V. (2003) Nomenclature of eudialyte-group minerals. *The Canadian Mineralogist*, **41**, 785–794.

Khomyakov A.P., Dusmatov V.D., Ferraris G., Gula A., Ivaldi G. and Nechelyustov G.N. (2003) Zirsilite-(Ce), $((Na,□)_{12}(Ce,Na)_3Ca_6Mn_3Zr_3Nb(Si_{25}O_{73})(OH)_3(CO_3){\cdot}H_2O$, and carbokentbrooksite, $((Na,□)_{12}(Na,Ce)_3Ca_6Mn_3Zr_3Nb(Si_{25}O_{73})(OH)_3(CO_3){\cdot}H_2O$ – two new eudialyte-group minerals from the Dara-i-Pioz alkaline massif, Tajikistan. *Zapiski Rossiiskogo Mineralogicheskogo Obshchestva* (*Proceedings of the Russian Mineralogical Society*), **132**, 40–51 [in Russian].

Khomyakov A.P., Nechelyustov G.N. and Rastsvetaeva, R.K. (2007) Aqualite, $(H_3O)_8(Na,K,Sr)_5Ca_6Zr_3Si_{26}O_{66}(OH)_9Cl$, a new eudialyte-group mineral from Inagli alkaline massif (Sakha-Yakutia, Russia), and the problem of oxonium in hydrated eudialytes. *Zapiski Rossiiskogo Mineralogicheskogo Obshchestva* (*Proceedings of the Russian Mineralogical Society*), **136**, 39–55 [in Russian].

Khomyakov A.P., Nechelyustov G.N. and Rastsvetaeva R.K. (2009) Voronkovite, $Na_{15}(Na,Ca,Ce)_3(Mn,Ca)_3Fe_3Zr_3Si_{26}O_{72}(OH,O)_4Cl{\cdot}H_2O$, a new mineral species of the eudialyte group from the Lovozero alkaline pluton, Kola Peninsula, Russia. *Geology of Ore Deposits*, **51**, 750–756.

Kim J., Schmitt U.W., Gruetzmacher J.A., Voth G.A. and Scherer N.E. (2002) The vibrational spectrum of the hydrated proton: Comparison of experiment, simulation, and normal mode analysis. *Journal of Chemical Physics*, **116**, 737–746.

Komatsuzaki T. and Ohmine I. (1994) Energetics of proton transfer in liquid water. I. Ab initio study for origin of many-body interaction and potential energy surfaces. *Chemical Physics*, **180**, 239–269, https://doi.org/10.1016/0301-0104(93)e0424-t.

Laria D., Martí J. and Guàrdia E. (2004) Protons in supercritical water: A multistage empirical valence bond study. *Journal of American Chemical Society*, **126**, 2125–2134, https://doi.org/10.1021/ja0373418.

Lebedev V.N. (2003) Sulfuric acid technology for processing of eudialyte concentrate. *Russian Journal of Applied Chemistry*, **76**, 1559–1563.

Lebedev V.N., Shchur T.E., Maiorov D.V., Popova L.A. and Serkova R.P. (2003) Specific features of acid decomposition of eudialyte and certain rare-metal concentrates from Kola Peninsula. *Russian Journal of Applied Chemistry*, **76**, 1191–1196.

Libowitzky E. (1999) Correlation of O–H stretching frequencies and O–H···O hydrogen bond lengths in minerals. *Monatshefte für Chemie*, **130**, 1047–1059.

Ma Y.Q., Stopic, S. Huang Z.Z. and Freidrich B. (2019) Selective recovery and separation of Zr and Hf from sulfuric acid leach solution using anion exchange resin. *Hydrometallurgy*, **189**, UNSP 105143.

Mandarino J.A. (1981) The Gladstone-Dale relationship. IV. The compatibility concept and its application. *The Canadian Mineralogist*, **41**, 989–1002.

McClellan A.L. and Pimentel G.C. (1960) *Hydrogen bond*. W.H. Freeman & Co Ltd, California Univ. 475 pp.

Novak A. (1974) Hydrogen bonding in solids correlation of spectroscopic and crystallographic data. Pp. 177–216 in: *Large Molecules*. Springer, Berlin-Heidelberg, https://doi.org/10.1007/BFb0116438.

Ortega I.K., Escribano R., Herrero V.J., Maté B. and Moreno M.A. (2005) The structure and vibration frequencies of crystalline HCl trihydrate. *Journal of Molecular Structure*, **742**, 147–152, https://doi.org/10.1016/j.molstruc.2005.01.005.

Paddison S.J. and Elliott J.A. (2005) Molecular modeling of the short-side-chain perfluorosulfonic acid membrane. *Journal of Physical Chemistry A*, **109**, 7583–7593, https://doi.org/10.1021/jp0524734

Pol'shin E.V., Platonov A.N., Borutsky B.E., Taran M.N. and Rastsvetaeva R.K. (1991) Optical and Mössbauer study of minerals of the eudialyte group. *Physics and Chemistry of Minerals*, **18**, 117–125.

Rastsvetaeva R.K., Chukanov N.V. and Aksenov S.M. (2012) *Eudialyte-Group Minerals*. Nizhny Novgorod State University, Nizhny Novgorod, 230 pp. [in Russian].

Sheldrick G.M. (2015) Crystal structure refinement with SHELXL. *Acta Crystallographica,* **C71**, 3–8.

Shtukenberg A. and Punin Yu.O.B. (2007) *Optically Anomalous Crystals*. Springer, Dordrecht, The Netherlands, 279 pp.

Sobolewski A.L. and Domcke W. (2002a) Hydrated hydronium: a cluster model or solvated electron? *Physical Chemistry Chemical Physics*, **4**, 4–10, https://doi.org/10.1039/b107373g.

Sobolewski A.L. and Domcke W. (2002b) *Ab initio* investigation of the structure and spectroscopy of hydronium-water clusters. *Journal of Physical Chemistry A*, **106**, 4158–4167.

STOE (2003) *WinXPow Version 2.08*. STOE & Cie GmbH, Darmstadt, Germany.

Vener M.V. and Librovich N.B. (2009) The structure and vibrational spectra of proton hydrates: $H_5O_2^+$ as a simplest stable ion. *International Reviews in Physical Chemistry*, **28**, 407–434. https://doi.org/10.1080/01442350903079955.

Vyas N.K., Sakore T.D. and Biswas A.B. (1978) The structure of 4-methyl-5-sulphosalicylic acid tetrahydrate. *Acta Crystallographica B*, **34**, 3486–3488, https://doi.org/10.1107/S0567740878011413

Zakharov V.I., Maiorov D.V., Alishkin A.R. and Matveev V.A. (2011) Causes of insufficient recovery of zirconium during acidic processing of Lovosero eudialyte concentrate. *Russian Journal of Non-Ferrous Metals*, **52**, 423–428.

https://doi.org/10.1180/mgm.2024.26 Published online by Cambridge University Press